

**Comparison of multiple AMBER force fields and development  
of improved protein backbone parameters**

**Table S1.** 28 Gly<sub>3</sub> conformers defined by the backbone dihedral angles  $\phi/\psi$  with corresponding QM energies relative to the conformer with lowest energy. Conformers are shown in ascending order of relative energies, the original conformer numbering is in the first column.

#	$\phi_1$	$\psi_1$	$\phi_2$	$\psi_2$	$\phi_3$	$\psi_3$	$\Delta E(\text{kcal/mol})$
1	80.79	-95.14	-87.29	62.02	80.47	-82.95	0.00
2	72.38	-108.34	-79.64	-18.51	-85.83	79.15	0.34
11	-81.91	79.48	59.59	-137.87	-85.47	3.46	0.40
17	-67.82	-24.81	-116.53	28.73	83.06	-83.57	1.96
3	141.37	-44.55	-84.79	73.26	69.01	-156.25	2.01
24	-71.66	-18.21	-121.16	36.82	71.79	-161.80	2.64
26	-77.11	-18.26	-86.54	62.61	117.03	-12.33	3.03
23	-84.62	74.62	-72.96	-17.15	-100.51	10.43	3.13
4	85.51	-69.73	85.94	-67.17	-85.25	66.67	3.18
6	85.35	-66.45	86.37	-65.29	86.02	-65.09	3.19
5	85.29	-74.96	-84.75	63.94	-86.46	63.34	3.25
13	-84.46	64.69	-61.40	133.19	97.54	-12.68	3.45
22	-61.86	137.72	119.83	-41.49	-69.75	171.68	3.80
15	-83.81	77.41	-95.19	-1.62	-85.25	67.95	4.30
19	84.57	-71.04	87.89	-58.77	-109.48	12.64	4.54
20	-60.54	136.10	98.22	-31.17	-107.88	-20.13	4.69
25	-92.08	-4.63	-85.33	69.43	-86.21	62.55	5.07
10	178.05	-177.66	-86.28	61.66	-87.01	65.00	5.29
8	175.03	-178.90	86.99	-64.84	-84.46	69.29	5.31
7	-176.01	178.89	-87.12	64.56	84.70	-68.27	5.33
21	172.52	-170.50	64.86	-131.93	-90.91	5.51	5.43
9	-180.00	179.94	-179.97	-179.89	-179.93	-179.91	5.67
18	82.88	-84.41	84.10	9.87	172.89	-178.15	5.70
12	178.70	-178.03	-177.52	178.28	-86.86	69.44	5.95
28	169.55	-168.86	-72.56	-17.62	-106.12	14.50	6.03
14	-86.93	79.35	-155.43	166.86	86.72	-68.54	6.30
16	89.01	-82.93	165.34	-173.27	178.94	179.34	6.96
27	179.36	-172.96	-87.47	-6.03	80.84	-156.31	8.05

**Table S2.** 51 Al<sub>3</sub> conformers defined by the backbone dihedral angles  $\varphi/\psi$  with corresponding QM energies relative to the conformer with lowest energy. Conformers are shown in ascending order of relative energies, the original conformer numbering is in the first column.

#	$\varphi_1$	$\psi_1$	$\varphi_2$	$\psi_2$	$\varphi_3$	$\psi_3$	$\Delta E(\text{kcal/mol})$
3	-90.38	67.70	69.56	-68.70	-63.54	131.49	0.00
1	62.01	-109.84	-70.19	-26.27	-85.91	80.17	0.40
2	-81.18	95.40	76.53	-54.39	-80.49	84.58	0.52
11	-68.34	-24.04	-68.52	-14.11	-96.13	3.52	0.55
15	57.63	-121.61	-65.59	-18.68	-96.38	4.77	0.71
4	-86.32	74.71	-88.49	71.35	-88.38	74.18	1.25
8	-82.42	79.87	52.39	-134.12	-84.78	-1.28	1.62
18	-84.82	80.48	-71.18	-21.41	-101.17	10.93	1.69
13	-84.31	81.74	-75.37	-26.60	-86.16	77.40	2.17
6	-159.02	157.42	-86.04	75.12	-88.29	75.79	2.67
14	-85.84	79.41	-123.29	11.98	-85.90	74.65	2.89
25	-83.96	81.81	-79.05	-16.51	-151.09	160.08	2.89
7	-158.65	161.67	-155.79	159.39	-85.44	81.14	3.07
16	-153.86	-128.98	-60.15	-35.38	-81.66	98.92	3.16
12	-66.50	131.48	75.12	-52.87	-94.54	-7.40	3.46
5	-157.76	163.19	-157.32	163.15	-156.26	161.27	3.49
10	-86.03	86.75	-157.42	155.97	-84.18	80.58	3.63
28	-81.69	-13.40	-153.68	159.79	-85.76	78.96	4.23
20	-156.82	166.95	-79.51	-15.18	-154.32	159.00	4.30
9	-72.57	-33.16	-91.15	55.80	-173.53	-44.26	4.50
40	72.89	-70.24	-58.06	135.39	62.69	24.18	4.67
34	-80.57	-15.30	-84.20	78.67	74.42	-59.71	4.88
42	61.27	36.57	74.65	-56.45	-86.46	-16.56	5.07
22	55.34	-128.81	-83.43	-5.62	76.06	-53.19	5.13
19	-87.95	50.37	-177.36	-40.74	-157.60	149.69	5.15
37	-156.19	157.71	-62.44	128.21	63.13	25.24	5.26
41	64.17	34.05	75.64	-53.19	-129.51	15.29	5.54
29	-155.21	156.07	56.72	-130.83	-87.20	-1.73	5.67
17	-85.97	77.63	-84.45	72.54	-171.51	-36.04	5.91
21	73.37	-70.05	-67.85	158.51	-158.63	157.89	6.00
38	-83.42	-10.26	-150.93	158.12	76.88	-47.88	6.50
26	-87.00	86.11	-148.36	145.72	76.26	-58.42	6.61
23	-155.75	165.70	-159.26	-61.61	-68.54	158.16	6.63
24	58.70	-120.69	-66.71	-29.58	-171.22	-56.07	7.22
27	-156.66	157.20	-83.56	72.67	-173.58	-35.27	7.45
32	76.23	-59.71	76.16	-54.76	75.42	-51.61	7.47
49	74.98	-54.40	56.49	43.73	72.51	-76.33	7.63
48	74.91	-70.66	63.03	33.96	-161.30	153.73	7.72
31	-164.53	-41.57	-155.93	158.58	-158.95	161.92	7.87
33	-156.75	159.97	-164.92	-45.06	-86.76	81.64	7.90
36	-166.31	-40.25	-153.47	156.11	-86.13	78.35	7.93
50	61.96	38.62	74.82	-59.25	77.85	-52.05	8.17
47	-166.11	-46.57	-85.92	82.50	-80.14	-19.63	9.13
39	76.09	-53.28	55.65	-140.65	-152.68	161.08	9.15
45	-166.27	-35.26	56.72	-131.56	-93.55	6.64	9.22
30	73.89	-74.61	-166.78	-46.53	-161.29	156.13	9.27
51	-150.68	-57.51	-71.52	-18.15	-93.00	2.38	9.33
46	-168.31	-40.10	75.58	-56.04	-85.76	75.31	9.43
35	-162.79	-59.14	-70.05	160.22	-86.43	79.15	9.76
43	-166.39	-44.87	-83.73	77.25	-175.92	-35.83	10.65
44	-163.05	-43.26	-153.08	144.43	75.00	-59.91	10.75

**Table S3.** The modification of the “parm99.dat” file supplied with the AMBER8 distribution is listed below in the form of a “frcmod” file (which is the format for applying small changes to “parm.dat” files, such as “parm99.dat”). This “frcmod” file will also be provided with the AMBER9 distribution.

---

```

from this paper.  Modifies parm99.
MASS

BOND

ANGL

DIHEDRAL
C -N -CT-C      1      0.00      0.0      -4.      four amplitudes and
C -N -CT-C      1      0.42      0.0      -3.      phases for phi
C -N -CT-C      1      0.27      0.0      -2.
C -N -CT-C      1      0.00      0.0      1.
N -CT-C -N      1      0.00      0.0      -4.      four amplitudes and
N -CT-C -N      1      0.55      180.0     -3.      phases for psi
N -CT-C -N      1      1.58      180.0     -2.
N -CT-C -N      1      0.45      180.0     1.
CT-CT-N -C      1      0.00      0.0      -4.      four amplitudes and
CT-CT-N -C      1      0.40      0.0      -3.      phases for phi'
CT-CT-N -C      1      2.00      0.0      -2.
CT-CT-N -C      1      2.00      0.0      1.
CT-CT-C -N      1      0.00      0.0      -4.      four amplitudes and
CT-CT-C -N      1      0.40      0.0      -3.      phases for psi'
CT-CT-C -N      1      0.20      0.0      -2.
CT-CT-C -N      1      0.20      0.0      1.

NONB

```

---

**Table S4.** For comparison, the following tables summarize the backbone torsional parameters for different variants of AMBER force fields discussed in the text and in this supplement. Even though it is hard to gain insights (even about the behavior of small peptides in solvent environment) from these values directly, it still provides some information about relative magnitudes and variations of amplitudes within each parameter set.

	ff03 <sup>a,1</sup>								ff96 <sup>2</sup>							
	$V_1$	$\gamma_1$	$V_2$	$\gamma_2$	$V_3$	$\gamma_3$	$V_4$	$\gamma_4$	$V_1$	$\gamma_1$	$V_2$	$\gamma_2$	$V_3$	$\gamma_3$	$V_4$	$\gamma_4$
$\phi$	1.02	0	0.35	$\pi$	0.23	0	–	–	0.85	0	0.30	$\pi$	0.00	0	0.00	0
$\psi$	0.68	$\pi$	1.45	$\pi$	0.46	$\pi$	–	–	0.85	0	0.30	$\pi$	0.00	0	0.00	0
$\phi'$	0.35	$\pi$	0.88	$\pi$	0.23	$\pi$	–	–	0.53	0	0.00	0	0.15	$\pi$	0.50	$\pi$
$\psi'$	0.78	$\pi$	0.07	$\pi$	0.06	0	–	–	0.00	0	0.07	0	0.00	0	0.10	0
$\phi''$	0.46	0	1.26	$\pi$	–	–	–	–								
$\psi''$	1.06	$\pi$	0.01	0	–	–	–	–								

<sup>a</sup> Additional backbone dihedral terms are present in ff03, defined as  $\phi''$  (C–N–C <sup>$\alpha$</sup> –H <sup>$\alpha$</sup> ) and  $\psi''$  (N–C–C <sup>$\alpha$</sup> –H <sup>$\alpha$</sup> ).

	ff99 <sup>3</sup>								ff99 $\phi$ <sup>4,5</sup>							
	$V_1$	$\gamma_1$	$V_2$	$\gamma_2$	$V_3$	$\gamma_3$	$V_4$	$\gamma_4$	$V_1$	$\gamma_1$	$V_2$	$\gamma_2$	$V_3$	$\gamma_3$	$V_4$	$\gamma_4$
$\phi$	0.80	0	0.85	$\pi$	0.00	0	0.00	0	0.00	0	0.20	$\pi$	0.00	0	0.00	0
$\psi$	1.70	$\pi$	2.00	$\pi$	0.00	0	0.00	0	1.70	$\pi$	2.00	$\pi$	0.00	0	0.00	0
$\phi'$	0.53	0	0.00	0	0.15	$\pi$	0.50	$\pi$	0.53	0	0.00	0	0.15	$\pi$	0.50	$\pi$
$\psi'$	0.00	0	0.07	0	0.00	0	0.10	0	0.00	0	0.07	0	0.00	0	0.10	0

	ff94 <sup>6</sup>								ff94 $\phi$ <sup>7</sup>							
	$V_1$	$\gamma_1$	$V_2$	$\gamma_2$	$V_3$	$\gamma_3$	$V_4$	$\gamma_4$	$V_1$	$\gamma_1$	$V_2$	$\gamma_2$	$V_3$	$\gamma_3$	$V_4$	$\gamma_4$
$\phi$	0.00	0	0.20	$\pi$	0.00	0	0.00	0	0.00	0	0.00	0	0.00	0	0.00	0
$\psi$	0.75	$\pi$	1.35	$\pi$	0.00	0	0.40	$\pi$	0.00	0	0.00	0	0.00	0	0.00	0
$\phi'$	0.53	0	0.00	0	0.15	$\pi$	0.50	$\pi$	0.53	0	0.00	0	0.15	$\pi$	0.50	$\pi$
$\psi'$	0.00	0	0.07	0	0.00	0	0.10	0	0.00	0	0.07	0	0.00	0	0.10	0

	ff99GA12 <sup>8</sup>								ff99mod2 <sup>9</sup>							
	$V_1$	$\gamma_1$	$V_2$	$\gamma_2$	$V_3$	$\gamma_3$	$V_4$	$\gamma_4$	$V_1$	$\gamma_1$	$V_2$	$\gamma_2$	$V_3$	$\gamma_3$	$V_4$	$\gamma_4$
$\phi$	0.40	4.58	0.41	5.29	0.02	5.02	0.02	5.81	1.00	0	0.00	0	0.00	0	0.00	0
$\psi$	0.48	4.78	0.45	5.39	0.12	5.76	0.45	5.52	0.70	$\pi$	1.10	$\pi$	0.00	0	0.00	0
$\phi'$	0.53	0	0.00	0	0.15	$\pi$	0.50	$\pi$	0.53	0	0.00	0	0.15	$\pi$	0.50	$\pi$
$\psi'$	0.00	0	0.07	0	0.00	0	0.10	0	0.00	0	0.07	0	0.00	0	0.10	0

**Figure S5.** The plots of  $\phi/\psi$  dihedral angles as a function of time in explicit water simulations of Ala<sub>3</sub> using ff99SB, ff03, ff94, ff99, ff94gs and ff99 $\phi$ . Replica exchange molecular dynamics (REMD) data for ff99SB and ff03 are also shown. Even though the enhanced sampling in REMD is apparent, the relative populations are unchanged compared to standard MD simulations. Time courses of dihedral angles plotted here demonstrate efficiency of sampling and justify presenting the populations in the form of free energy dihedral maps. Distinct features of some forcefields are readily visible: ff99SB has the highest population of  $\alpha_L$  region ( $\phi \approx 40^\circ$  to  $80^\circ$ ); ff94 and ff99 are mostly helical ( $\psi$  only ranges from  $-60^\circ$  to  $40^\circ$ ); ff99 is the only forcefield with two distinct basins in  $\alpha$ -region ( $\phi$  around  $-50^\circ$  but also around  $-140^\circ$ );  $\alpha$ -helical region in ff94gs is shifted to lower  $\psi$  (around  $-45^\circ$ ) compared to all other forcefields ( $\psi \approx -30^\circ$  to  $10^\circ$ ). All those features can be also seen in the free energy maps (Figure 3 in the main text).

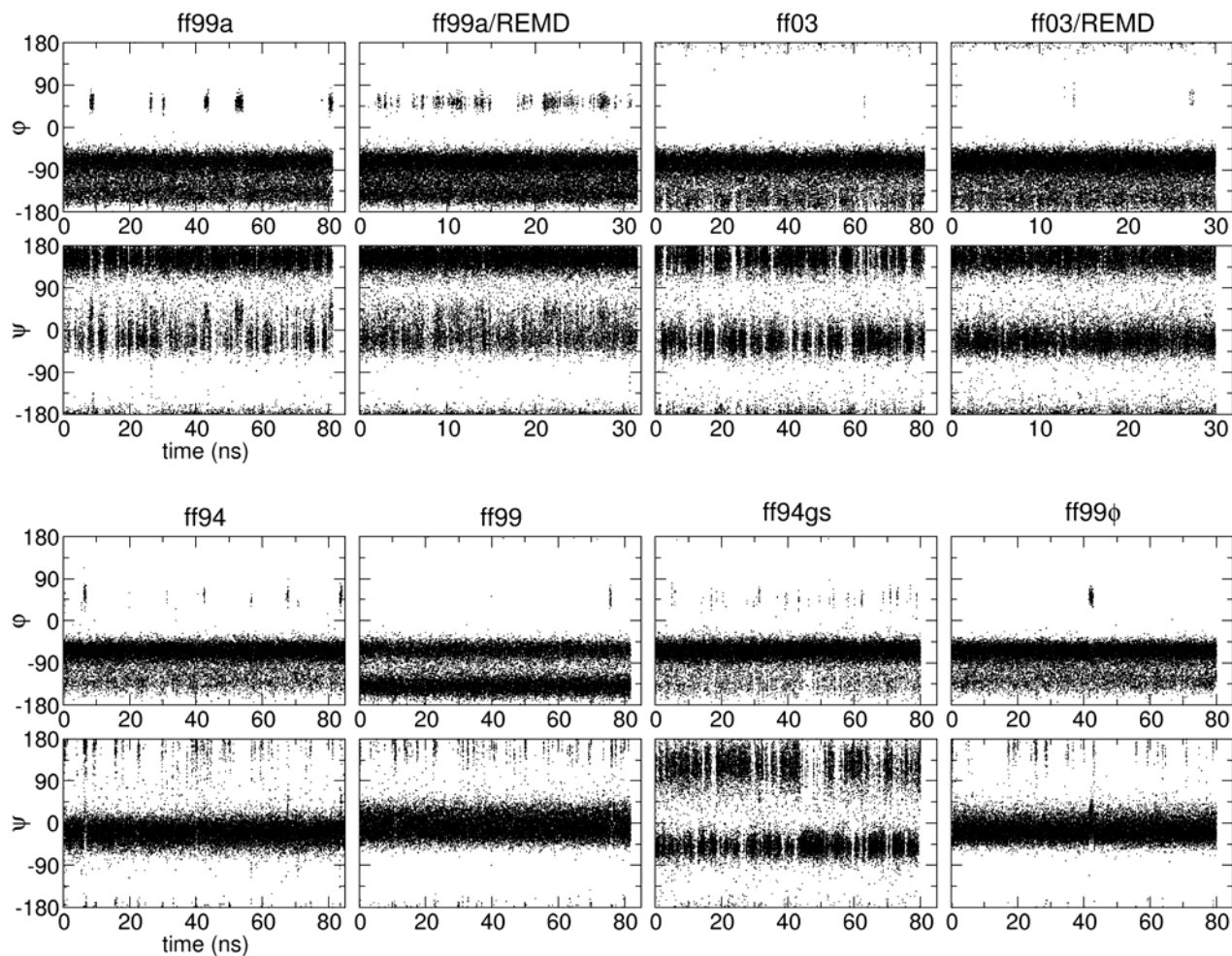
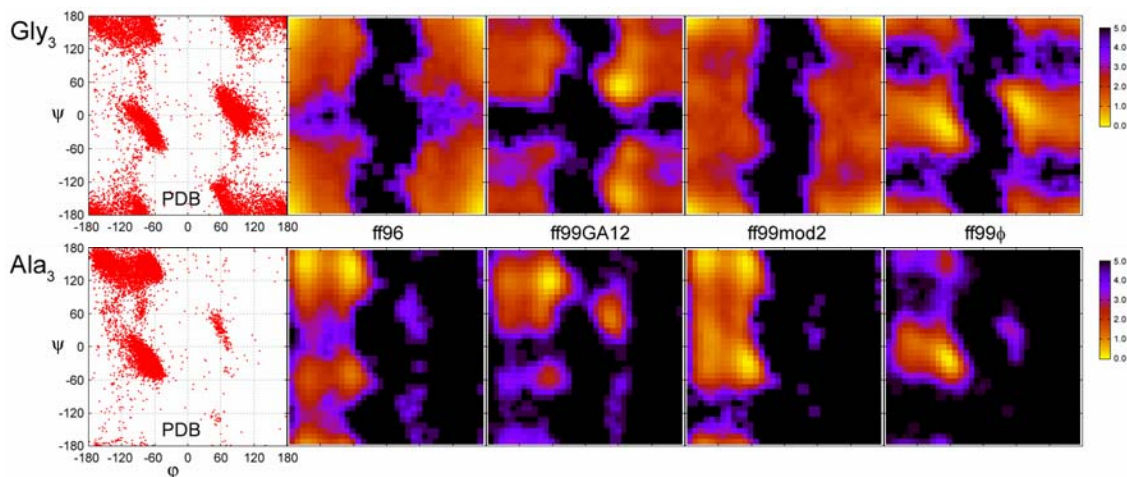


**Figure S6.** The plots of remaining forcefields we tested, shown in the form of free energy plots extracted from 80 ns explicit water simulations of Gly<sub>3</sub> and Ala<sub>3</sub>. The axis description and energy levels are the same as in Figure 3 in the main text. For example, it is fairly obvious from ff96 plot why it is considered to prefer extended  $\beta$ -like structures, as this is the region that it primarily samples. ff99GA12<sup>8</sup> also samples mainly  $\beta$ -structures but also has a significant stabilization for  $\beta$ -turns (positive  $\phi/\psi$  region). We have shown previously that in conjunction with Generalized Born model, the insufficient sampling for  $\alpha$ -region and GB bias for  $\alpha$ -region actually restore a reasonable balance between  $\beta$ - and  $\alpha$ -structures for ff99GA12. ff99mod2<sup>9</sup> Ala<sub>3</sub> plot looks quite reasonable but, as is also the case for ff96 and ff99GA12, has inadequate glycine sampling due to incorrect procedure of backbone parametrization (which was explained in the main text). ff99 $\phi$  looks very similar to ff94 and thus inherits over stabilization of  $\alpha$ -helical region.



## References:

1. Duan Y, Wu C, Chowdhury S, Lee MC, Xiong GM, Zhang W, Yang R, Cieplak P, Luo R, Lee T, Caldwell J, Wang JM, Kollman P. A point-charge force field for molecular mechanics simulations of proteins based on condensed-phase quantum mechanical calculations. *J Comput Chem* 2003;24(16):1999-2012.
2. Kollman P, Dixon R, Cornell W, Fox T, Chipot C, Pohorille A. The development/application of the "minimalist" organic/biochemical molecular mechanic force field using a combination of ab initio calculations and experimental data. In: van Gunsteren WF, Weiner PK, Wilkinson AJ, editors. *Computer Simulations of Biomolecular Systems. Volume 3.* Dordrecht, The Netherlands: Kluwer Academic Publishers; 1997. p 83-96.
3. Wang JM, Cieplak P, Kollman PA. How well does a restrained electrostatic potential (RESP) model perform in calculating conformational energies of organic and biological molecules? *J Comput Chem* 2000;21(12):1049-1074.
4. Sorin EJ, Pande VS. Empirical force-field assessment: The interplay between backbone torsions and noncovalent term scaling. *J Comput Chem* 2005;26(7):682-690.
5. Sorin EJ, Pande VS. Exploring the helix-coil transition via all-atom equilibrium ensemble simulations. *Biophysical Journal* 2005;88(4):2472-2493.
6. Cornell WD, Cieplak P, Bayly CI, Gould IR, Merz KM, Ferguson DM, Spellmeyer DC, Fox T, Caldwell JW, Kollman PA. A Second Generation Force Field For the Simulation of Proteins, Nucleic Acids, and Organic Molecules. *Journal of the American Chemical Society* 1995;117(19):5179-5197.
7. Garcia AE, Sanbonmatsu KY.  $\alpha$ -Helical stabilization by side chain shielding of backbone hydrogen bonds. *Proceedings of the National Academy of Sciences of the United States of America* 2002;99(5):2782-2787.
8. Okur A, Strockbine B, Hornak V, Simmerling C. Using PC clusters to evaluate the transferability of molecular mechanics force fields for proteins. *J Comput Chem* 2003;24(1):21-31.
9. Simmerling C, Strockbine B, Roitberg AE. All-atom structure prediction and folding simulations of a stable protein. *Journal of the American Chemical Society* 2002;124(38):11258-11259.